AAS 25-428

CISLUNAR INITIAL ORBIT DETERMINATION AND TARGET TRACKING USING KINEMATIC FITTING AND PARTICLE GAUSSIAN MIXTURE FILTERING*

Ishan P. Paranjape† and Suman Chakravorty‡

In this work, we present a method for probabilistic initial orbit determination (IOD) and orbit determination (OD) which attempts to minimize the number of assumptions for producing target state parameters while providing a robust tracking method in cislunar space. Since targets in cislunar space tend to stay within an observer's field of view for long periods of time, we propose a method for producing an initial state estimate for our object using kinematic fitting of observations from our measurement model. Once an initial state estimate is formed, we utilize the powerful Particle Gaussian Mixture (PGM) Filter to propagate our initial state estimate and update with observations over a long period of time. This combined IOD/OD framework allows us to generate an initial state estimate for a target with minimal assumptions and to sufficiently address the highly nonlinear natures of our target's motion and of our measurement model.

INTRODUCTION

The extension of space situational awareness (SSA) capabilities into cislunar space is a key objective of the National Cislunar Science and Technology Strategy. Specifically, there exists a need to identify and detect colliding objects and/or potentially dangerous spacecraft operations or space weather elements in order to ensure safe operation of spacecraft within this domain.[1] Since the volume of the cislunar domain is nearly a thousand-fold that of the volume of orbits below the geocentric (GEO) limit, and a large share of Resident Space Objects (RSOs) – also referred to more generally as targets – exist within this domain, effective cislunar target tracking becomes a crucial problem. Furthermore, with the rise of lunar missions such as that of China's Chang'e-5 and India's Chandrayaan, it becomes even more imperative to ensure the safe operation of spacecraft and facilitate space traffic coordination efforts in the cislunar domain. One of the ways we can ensure this safe operation is by initializing and maintaining custody of spacecraft and RSO orbits using initial orbit determination (IOD) and orbit determination (OD) for target tracking.

The goal of IOD in a single target tracking scenario is to combine several measurements of a single RSO and then to fit a state vector through the measurements.[2] While one of the most well-known methods of IOD is Gauss's Method, more specialized IOD methods such as constrained admissible region (CAR) and probabilistic admissible region (PAR) persist throughout literature.[3–7]

†Graduate Assistant - Research, Department of Aerospace Engineering, Texas AM University, 710 Ross St., College Station, TX 77843.

‡Professor, Department of Aerospace Engineering, Texas AM University, 710 Ross St., College Station, TX 77843.

Mishra et. al. 2024 utilize PAR to generate initial estimates of a target within regimes up to geosynchronous orbit (GEO), the point up to where the effects of the two-body problem are valid. More specifically, their IOD framework involves postulating statistics about four of the six major orbital elements as *a priori* information and generating multiple observations of the target state using those statistics.[8] Along with two angular measurements, an initial state estimate is formulated. *Bolden et. al. 2022* and *Griggs et. al. 2023* utilize PAR to generate a similar set of initial orbit estimates.[9,10] Since traditional orbital elements cannot be used effectively in the cislunar domain, where effects of the three-body problem dominate, the authors rely upon postulated statistics of the range utilizing light intensity curves generated by *Hejduk 2013*, sensor movement constraints for angular rates, and the singular constant of integration (Jacobi's constant) produced by the equations of motion of the circular-restricted three-body problem (CR3BP).[11] *Mishra et. al. 2024*, *Bolden et. al. 2024*, and *Griggs et. al. 2023* all utilize the same OD framework: the Particle Gaussian Mixture (PGM) Filter.[8,12]

While *Bolden et. al. 2022* and *Griggs et. al. 2023* provide an effective method for IOD with PAR, their method relies on postulating several statistics, resulting in lots of *a priori* information required beforehand. One of the reasons Gauss's method for orbit determination remains a popular benchmark for IOD is its limited use of assumptions and the simplicity associated with obtaining an initial state estimate of an RSO up to the GEO regime by using three consecutive short-arc measurements. Although we cannot yet apply Gauss's method to the cislunar domain, we may be able to perform probabilistic IOD and target tracking with fewer initial information and postulated statistics. In this work, we seek to perform IOD and OD in the cislunar domain under minimal assumptions through kinematic fitting of our observations and using the PGM framework for target tracking. For IOD, we shall specifically make use of the fact that RSOs in the cislunar domain remain within the line of sight of an observer for extended periods of time, allowing us to determine the object's position for an extended period of time.

The remainder of this paper is organized as follows. First, we introduce our combined IOD and OD framework, which leverages a nonlinear dynamics model and a nonlinear measurement model. Then, we present two different examples with our combined IOD/OD framework and compare the performance of our OD framework with another nonlinear filtering method. Finally, we present possible extensions to our IOD and target tracking framework.

CISLUNAR IOD/OD FRAMEWORK

For effective target tracking in the cislunar domain, we require an IOD method to generate an initial state estimate and an OD method for continuous tracking and maintaining custody of our RSO. In near-Earth regimes (i.e. LEO, GEO) governable by the two-body problem, targets move relatively quickly due to the force of gravitational attraction induced by the Earth on the RSO, allowing observers or sensors only a brief glimpse of the RSO trajectory. Due to the vastness of the cislunar domain, an RSO may appear in the observer's line of sight (or sensor field of view) for several hours at a time, meaning that we can make several consecutive observations. We are only limited by the fact that the Earth's spin will allow an observer to observe an RSO in cislunar space for about 10-20 hours before the RSO disappears over the horizon. Nevertheless, those hours-long passes are much longer than the minutes-long passes of RSOs up to the GEO limit. Because of this, we can piece through several consecutive observations to effectively estimate the state of a target at a given point in time. Before we describe this IOD method in greater detail, we shall outline the dynamics and measurement models we shall use for our state estimation framework.

Dynamics Model

Beyond the GEO regime, it becomes difficult to model RSO dynamics with the two-body problem. At that point, effects of larger gravitational bodies such as the Moon and the Sun become apparent, and the use of Keplerian orbital elements start to become obsolete. Nevertheless, multiple dynamics models exist for bodies in cislunar space. The most popular of these models is the circular-restricted three-body problem (CR3BP).[13] The dynamics of the CR3BP are expressed in a reference frame centered around the center of mass of the two largest orbiting bodies, which orbit about their center of mass (also referred to as the barycenter) in a circular motion. For the cislunar domain, these two large orbiting bodies are the Earth and the Moon. The RSO is generalized as a third body with negligible mass relative to the other two bodies. The equations of motion of the target with respect to this barycentric frame are given below.

$$\ddot{x} = x + 2\dot{y} - \frac{(1-\mu)(x+\mu)}{r_1^3} - \frac{\mu x - \mu(1-\mu)}{r_2^3} \tag{1a}$$

$$\ddot{y} = y - 2\dot{x} - \frac{(1-\mu)y}{r_1^3} - \frac{\mu y}{r_2^3} \tag{1b}$$

$$\ddot{z} = \frac{(1-\mu)z}{r_1^3} - \frac{\mu z}{r_2^3} \tag{1c}$$

In the equations above, x and y define the orbital plane of the Earth and the Moon, r_1 and r_2 define the distance between the target and the centers of masses of bodies 1 and 2, respectively. μ is a mass parameter that defines the weights of the two major bodies relative to each other, and is assumed constant. All mass, time, and distance quantities are expressed in non-dimensional units. *Schaub and Junkins 2003* describe these non-dimensional units in more detail.[13]

Measurement Model

A traditional radar or optical sensor provides measurements of azimuth, elevation, and, at times, range. Due to the vast distances associated with cislunar space, range measurements are not always accurate, whereas angular measurements are much more reliable. For this reason, our measurement model's noise statistics for range encompass a significant enough fraction of the true range value, while the angular noise statistics are kept very low due to the high fidelity of current optical and radar sensors. The following set of equations relate range, azimuth, and elevation with state coordinate components in an observer-centered topocentric reference frame.

$$R = \sqrt{x^2 + y^2 + z^2} \tag{2a}$$

$$AZ = tan^{-1}(\frac{y}{x}) \tag{2b}$$

$$EL = \frac{\pi}{2} - cos^{-1}(\frac{z}{\sqrt{x^2 + y^2 + z^2}}) \tag{2c}$$

Similarly, we can convert our measurement model's components to obtain components of our target state in the topocentric frame.

$$x = R * cos(AZ) * cos(EL) \tag{3a}$$
$$y = R * sin(AZ) * cos(EL) \tag{3b}$$
$$z = R * sin(EL) \tag{3c}$$

Although we assume that range is detectable for this measurement model, most radar and optical telescopic sensors make use of angles-only measurements. In some of the aforementioned studies of IOD in cislunar space, scientists have used PAR to postulate statistics about parameters from which one can infer the target state.[9,10] These studies make use of the equations of a diffuse/specular sphere's light intensities, derived from an experimental study by *Hejduk 2013*.[11] By postulating statistics about the albedo-area product and solar phase angles, it is possible to derive several values for the range using the PAR technique. For this study, however, we shall assume that range is a component (although less reliable than azimuth or elevation angles) of our measurement vector.

Initial Orbit Determination

By obtaining measurements of the range, azimuth, and elevation, one can effectively estimate the position of a target in the topocentric reference frame using Eqs. 3. Since RSOs in cislunar space are unlikely to leave the field of view of the sensor site for several hours at a time, one may be able to obtain a time-series data of $x(t)$, $y(t)$, and $z(t)$ over a 10-20 hour period. Since we can program or simulate an optical sensor to take measurements as frequently as every minute to every hour, we obtain a time-series data of the position $\mathbf{r}(t) = [x(t), y(t), z(t)]^T$ with several points. We may then be able to fit a polynomial of some small order (usually not greater than four) through $x(t)$, $y(t)$, and $z(t)$ as some kinematic functions of time only. Once proper fitting coefficients have been obtained using curve fitting methods such as least squares, it is possible to find an approximation of the velocity components $\mathbf{v}(t)$ using simple calculus.

$$\mathbf{v}(t) = \frac{d}{dt}\mathbf{r}(t) = [\frac{dx}{dt}, \frac{dy}{dt}, \frac{dz}{dt}]^T \tag{4}$$

By combining $\mathbf{r}(t)$ and $\mathbf{v}(t)$, we have a time-series estimate of the state of our target in the topocentric frame. Since we wish to utilize several measurements during a single pass of the target over the sensor field of view (also referred to as the line of sight), it behooves us to only utilize part of the pass as our interpolation interval. To show that this IOD framework works for CR3BP orbits, we include Figure 1, which compares fitted 3rd and 4th order polynomials for all six components of the system state with their true values, assuming noiseless data.

If we sample from from our noise statistics a large number of measurements resulting in time-series signals of noisy data, we shall obtain several different points for $x(t)$, $y(t)$, $z(t)$, $\dot{x}(t)$, $\dot{y}(t)$, and $\dot{z}(t)$ in the topocentric frame. While a single state vector may not accurately capture the target's true state or truth, a large number of measurement samples and kinematic fits will generate a large point cloud (or a family of orbits) within which the truth may be accurately captured. An example of such a point cloud is presented in Figure 2.

With this simple IOD framework, we have a solid initial state estimate (or orbit) from which we can keep track of the target regardless of whether or not we can take measurements at a particular time step. In the proceeding subsection, we shall explain the filtering technique which we utilize for orbit determination.

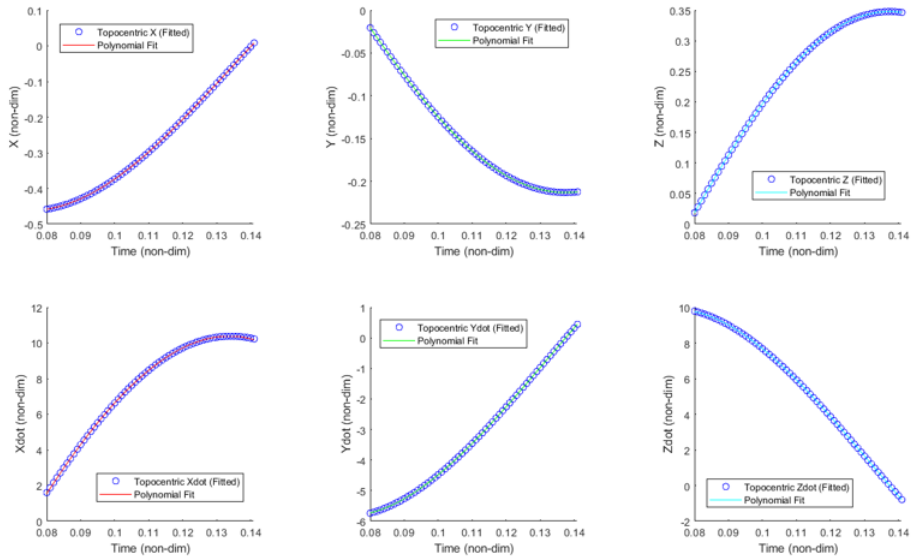

Figure 1: Polynomial fitting over half (50%) of an object's pass over the sensor FOV. Using multiple calculations of $\mathbf{r}(t)$ from the measurement model, one can fit a fairly accurate 3rd or 4th order polynomial as a function of t, take their derivatives, and obtain a fairly accurate set of fitted polynomials for $\mathbf{v}(t)$.

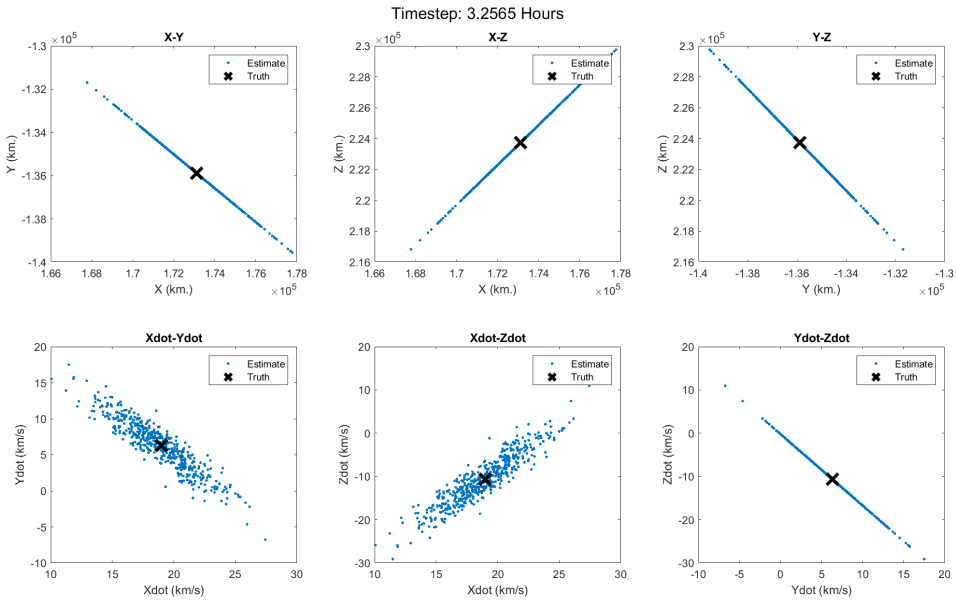

Figure 2: The final result of our IOD framework is encapsulated within this particle cloud (in blue), within which the target's true state (given as an orange plus sign) lies. This is the result of fitting several signals of time-series data derived from noise statistics.

Orbit Determination

Proper orbit determination of a highly nonlinear system coupled with a highly nonlinear measurement model requires a sophisticated filter. Due to the high noise statistics associated with the range measurement and the relative accuracy of the azimuth and elevation measurements, simple filters such as an Extended Kalman Filter (EKF) or an Unscented Kalman Filter (UKF) may fail to accurately capture the non-Gaussian nature of the initial estimate or posterior estimates thereafter. For this reason, it is better to model the IOD results and estimates thereafter using a Gaussian Mixture Model (GMM).

For our OD framework, we shall continue to use the recursive Particle Gaussian Mixture (PGM) filter developed by *Raihan & Chakravorty 2018* and applied by *Bolden et. al. 2022* and *Griggs et. al. 2023*. Unlike traditional particle filters, the PGM filter has a clustering step which groups particles propagated nonlinearly from an *a priori* distribution into a GMM. These clusters each have an assigned weight and an associated mean vector and covariance matrix. With the observation from our sensor, we may be able to update each cluster's mean vectors, covariance matrices, and weights. The following time step will use Markov Chain Monte Carlo (MCMC) sampling to draw from this posterior distribution. This powerful resampling step makes the PGM filter more robust to nonlinear dynamics or measurement models, whereas traditional nonlinear filters are subject to particle depletion step at the update step. The Particle Gaussian Mixture algorithm is detailed in Algorithm 1, copied from Ref. [12].

Algorithm 1 Particle Gaussian Mixture Filter Algorithm

- Given $\pi_0(x) = \sum_{i=1}^{M(0)} \omega_i(0) p_g(x; \mu_i(0), P_i(0))$, transition density kernel $p(x'|x)$, $n = 1$.
  1. Sample N_p particles from π_{n-1} and the transition density kernel $p_n(x'|x)$ as follows:
     - Sample $X^{(i)'}$ from $\pi_{n-1}(.)$.
     - Sample $X^{(i)}$ from $p(.|X^{(i)'})$.
  2. Use a clustering algorithm $\mathcal{C}$ to cluster the set of particles $X^{(i)}$ into $M^-(n)$ Gaussian clusters with weights, mean, and covariance given by $\{\omega_i^-(n), \mu_i^-(n), P_i^-(n)\}$.
  3. Update the mixture weights and mixture means and covariances to $\{\omega_i^+(n), \mu_i^+(n), P_i^+(n)\}$, given the observation z_n, utilizing the Kalman update.
  4. $n = n + 1$. Go to Step 1.

RESULTS AND DISCUSSION

In this section, we shall demonstrate the utility of our combined IOD-OD framework using two examples. For the first example, we choose a relatively stable orbit with a sensor tasked to take measurements at a sufficiently high frequency. We apply our combined framework over a period longer than three weeks to demonstrate the long-term utility of the PGM filter. For our second example, we modify our measurement model while applying our IOD-OD framework to a more chaotic orbit, demonstrating a scenario where PGM may outperform other, more traditional filters.

To quantize the uncertainty of our PGM filter's estimate over time, we introduce an entropy metric $E(k)$ outlined in *Mishra et. al. 2024*, given below.[8]

$$E(k) = \log \sum_{i=1}^{N} \omega_i^+ |\mathbf{P}_{xx,k}^{(i)+}| \tag{5}$$

Since we calculate the entropy after the PGM update step, ω_i^+ represents the posterior GMM component weights, and $|\mathbf{P}_{xx,k}^{(i)+}|$ represents the determinant of the posterior covariance matrix for each component i. Since the product of all GMM components $\omega_i^+ |\mathbf{P}_{xx,k}^{(i)+}|$ becomes large as the number of clusters increase, it makes more sense to utilize a log-sum approach.

Example 1

About a decade ago, the Interstellar Boundary Explorer (IBEX) spacecraft entered a range of highly elliptic orbits around Earth such that it was in 3:1 resonance in the Earth-Moon system.[14] *Dichmann et. al. 2013* examines three classes of resonant orbits relevant to IBEX's cislunar trajectories.[15] For this example, we focus upon the planar mirror orbit. It is classified as such due to its initial position located on the CR3BP x-axis and its initial velocity only has a y-component and is hence perpendicular to the x-axis. All trajectories are in the Earth-Moon CR3BP $x - y$ plane for simplicity. We chose this orbit due to its relatively short, periodic nature, spanning roughly 27 days. Figure 3 provides a graphical representation of this orbit.

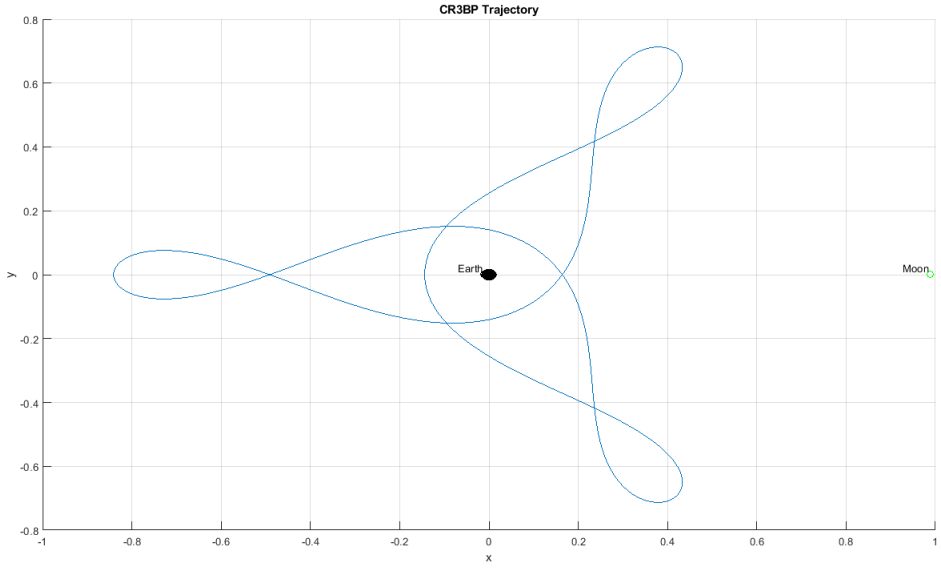

Figure 3: The planar mirror orbit described by *Dichmann et. al. 2013* depicting a periodic orbit in the Earth-Moon system in the barycentric reference frame. All distance units in this figure are normalized in accordance with the CR3BP equations of motion.

Starting with the initial state estimate produced in Figure 2, we may recursively propagate, cluster, and update our cluster until the end of the first pass of the RSO. With the clustering method outlined in *Mishra et. al. 2024*, we utilized six clusters for our propagation and update steps.[8,16] The *a priori* estimate (i.e. after propagating by one time step and clustering into six clusters) of the target state is given by Figure 4.

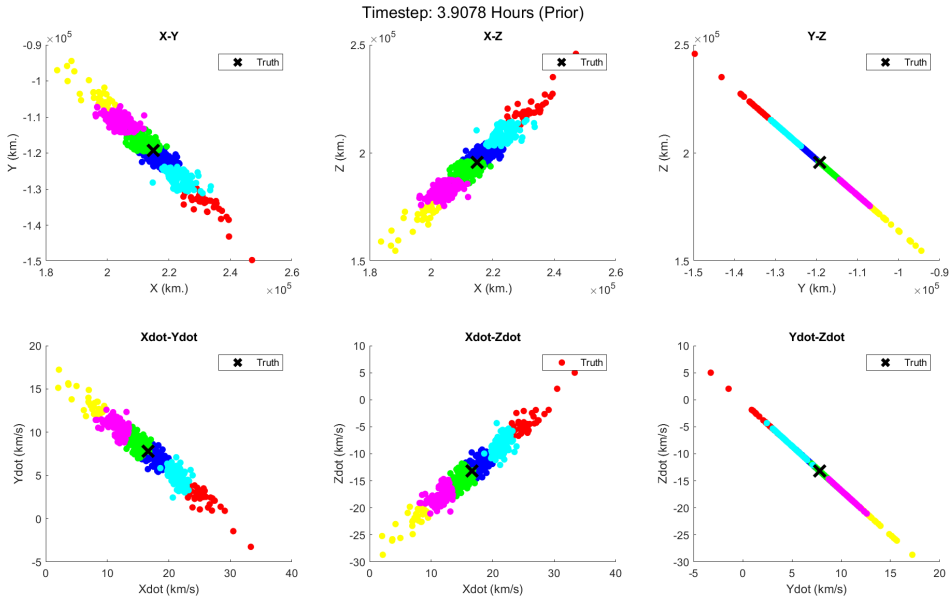

Figure 4: After our IOD step, we propagate each particle using our dynamics model and cluster using the k-means algorithm.[8,12,16] The resulting distribution, modeled as a Gaussian mixture model, becomes our new *a priori* distribution. The expectation is that the truth (indicated by a black cross) will lie somewhere at the intersection of the blue and green clusters after the update step.

We utilize the Kalman update to obtain our new GMM, sample several hundreds or thousands of points from this distribution, and repeat the filtering process for our desired length of time. Figure 5 shows the posterior distribution of our PGM filter.

At one point, the RSO exits our sensor FOV, and we propagate a large number of particles drawn from a posterior distribution at the end of the first pass. As we propagate all of the particles to the time at which the RSO first reappears in our line of sight (i.e. the beginning of the second pass), the state estimate covariances continue to consistently encapsulate the target truth. Eventually, once the RSO reenters the sensor's FOV, we propagate, cluster, and update with our PGM filter to obtain the result shown in Figure 6. Focusing on the top left plots of Figures 5 and 6, the standard deviation of the posterior distributions are reduced by a factor of almost 20 in the topocentric y-direction.

Beyond a certain point, as demonstrated by *Mishra et. al. 2024*, it is possible to switch from a PGM filter to an Ensemble Kalman Filter (EnKF). For this example, we utilized a PGM filter up to the beginning of the fourth pass, at which point our entropy had reduced significantly and allowed us to more robustly model our resulting particle distributions as a single-component Gaussian PDF. Figures 7 and 8 show the first and last points (also the final step of our simulation) at which we use an EnKF, respectively.

By observing the range of all six axes between Figures 4 to 8, it is clear that as the PGM filter is applied, the size of the particle clouds (and hence the entropy) is reduced. Figure 9 shows how entropy reduces with each step of the PGM and/or EnKF filters. In the proceeding example, we explore an orbit in which a PGM filter must be used as opposed to an EnKF in order to successfully track a target for a long period of time with no observations.

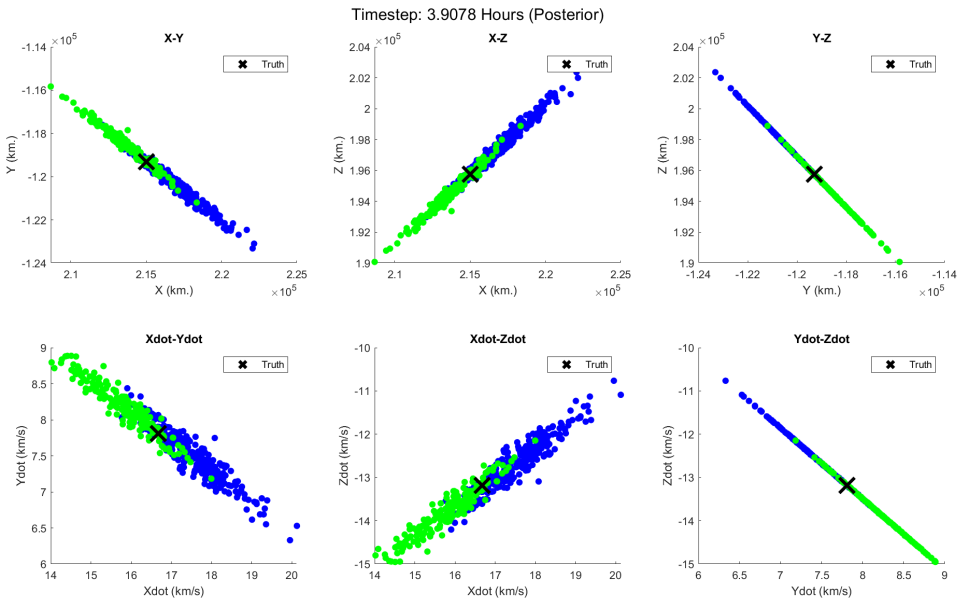

Figure 5: As expected, our Kalman update step filters out four of our six original clusters and leaves us with the green and blue clusters, the intersection between which lies the truth. The particles shown above are drawn from the posterior distribution and projected.

Example 2

The Earth-Moon axial Lagrange points have long interested the astrodynamics community due to the instability of the equilibrium points. The area around these Lagrange points enables spacecraft in cislunar space for more efficient orbit plane changes and transfers compared to a standard Hohmann transfer. The L_2 Lagrange point in particular has intrigued scientists because of the myriad of bifurcations and orbit families generated with short position perturbations in the barycentric x-direction and short velocity perturbations in the barycentric y-direction.[17–19] Since our IOD-OD framework uses a probabilistic, particle-based approach with small time differences between consecutive observations, several bifurcations or differing orbit families are not readily visible with the current OD framework.

In order to observe the chaotic orbit behaviors using our particle-based approach, we make several modifications to the first example. First, we choose an initial condition such that, when propagated for about 48 hours, passes through or near the L_2 Lagrange point at some velocity close to zero in the barycentric y-direction. This would allow our sensor to make a sufficient number of observations to reduce the uncertainty of our target estimate. Additionally, we modify our measurement model to angles-only (i.e. we only consider AZ and EL measurements and discard range measurements for OD altogether). For the first 48 hours of our modified orbit determination framework, we take measurements roughly once every 40 minutes and filter using the EnKF. After that, we do not take any measurements for about 8 days and propagate several particles drawn from the posterior distribution at the 48-hour mark for that length of time. The distribution of particles is shown in Figure 10.

During that eight-day period with pure propagation and no observations, a small bifurcation re-

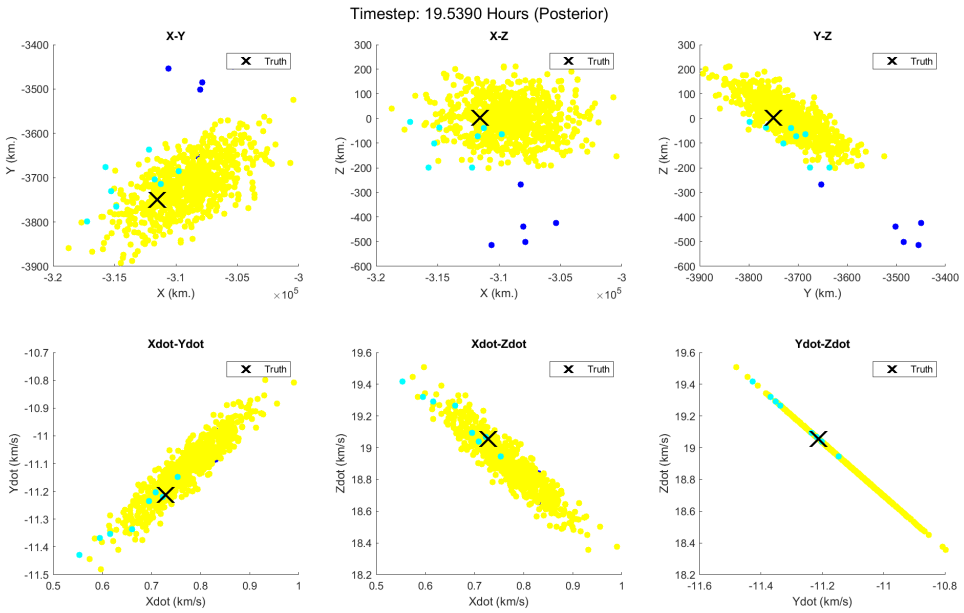

Figure 6: At the beginning of the second pass, the covariance of our state estimate greatly decreases after the update step, resulting in posterior GMM whose weight is given overwhelmingly to a single cluster encapsulating the truth. With subsequent observations, the size of our particle cloud will continue to shrink.

sults in two orbit families, the larger one in which the truth is contained. The bimodality of this PDF and the curvature of the particle distributions of both modes in the position and velocity spaces require a filter such as the PGM, which can approximate complex *a priori* estimates better than an EnKF. Figures 11 and 12 show what happens at the update step when a PGM filter is used and when an EnKF is used, respectively.

While several orbits in cislunar space governed by CR3BP dynamics are relatively stable, and a high frequency of observations may justify using an EnKF as opposed to the PGM framework, more chaotic orbits with lower observation frequencies will require a PGM filter due to the non-Gaussian nature of *a priori* estimates.

CONCLUSIONS AND FUTURE WORK

In this paper, we proposed a new IOD framework which involved fitting a polynomial through series of range, azimuth, and elevation angle observation data to obtain an initial state estimate. Then, due to the nonlinearity of cislunar dynamics and our measurements, we presented an OD framework in the form of the PGM filter, which is robust to both stable and unstable cislunar orbits. We demonstrated the use of PGM on two different orbits and demonstrated the superiority of the PGM filter over an EnKF for robustness to orbits which yield unwieldy state estimates. This combined framework will assist with tracking targets in cislunar space over the long term.

There are several improvements and extensions that we wish to make to this work. We wish to examine the performance of the PGM filter and an EnKF for relatively stable cislunar orbits.

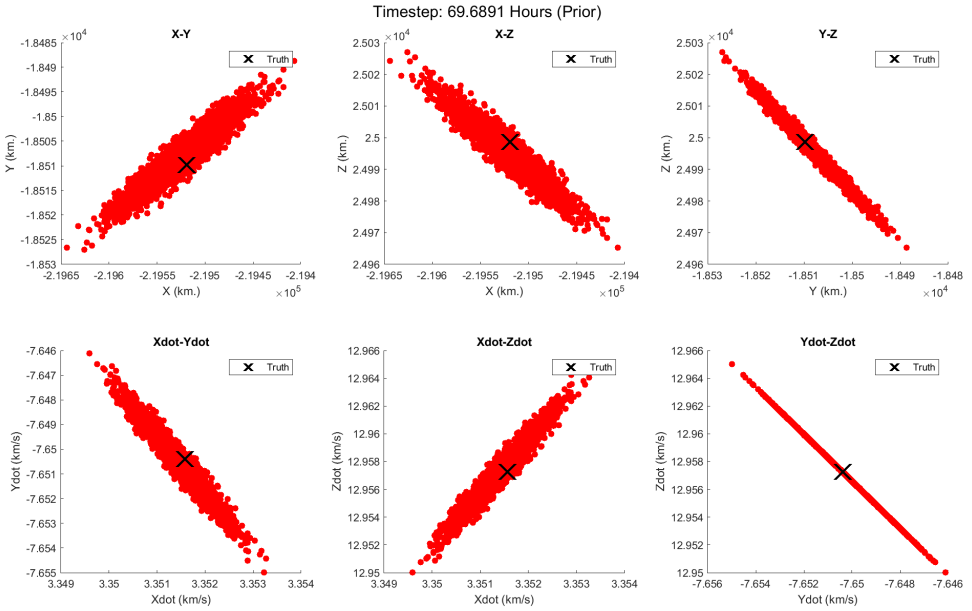

Figure 7: The particle estimate of our PGM filter at the beginning of the fourth pass, at which point we transition to an EnKF for the remainder of the simulation

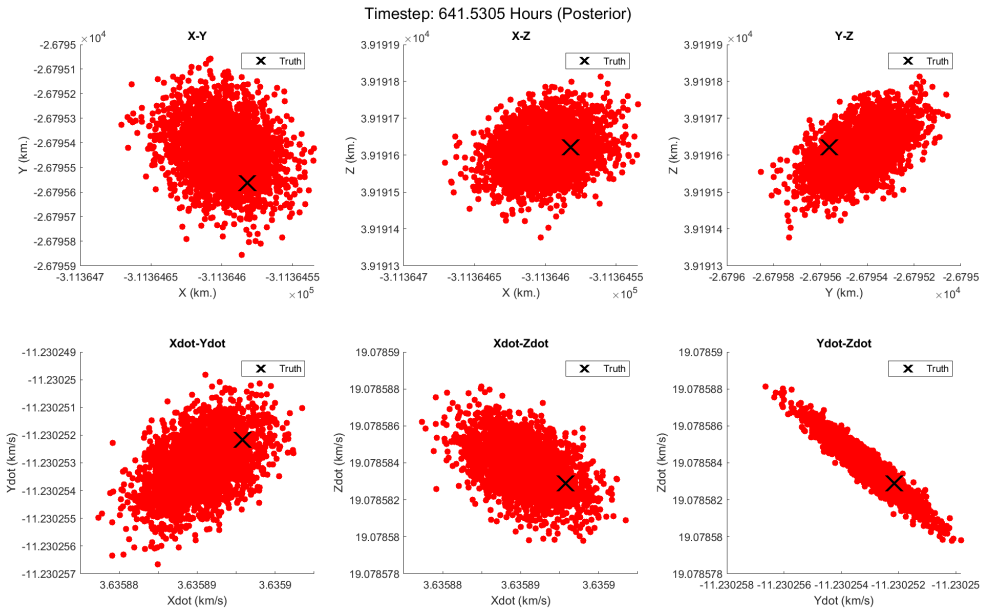

Figure 8: The particle estimate of our hybrid PGM-EnKF simulation after about 27 days, at which point we have tracked a target for a full period of *Dichmann et. al. 2013*'s planar mirror orbit

Although we have demonstrated our combined IOD-OD framework for some chaotic orbits, we

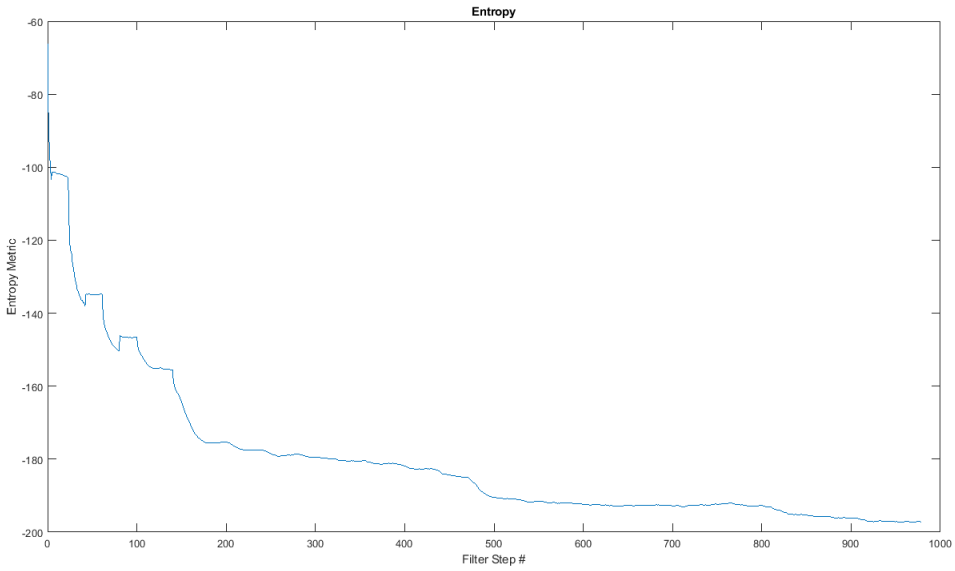

Figure 9: The entropy evolution at each filtering step. After three regions of relatively flat entropy changes (indicating the steps in between target passes), we switch from a PGM to an EnKF and continue through the end of the simulation.

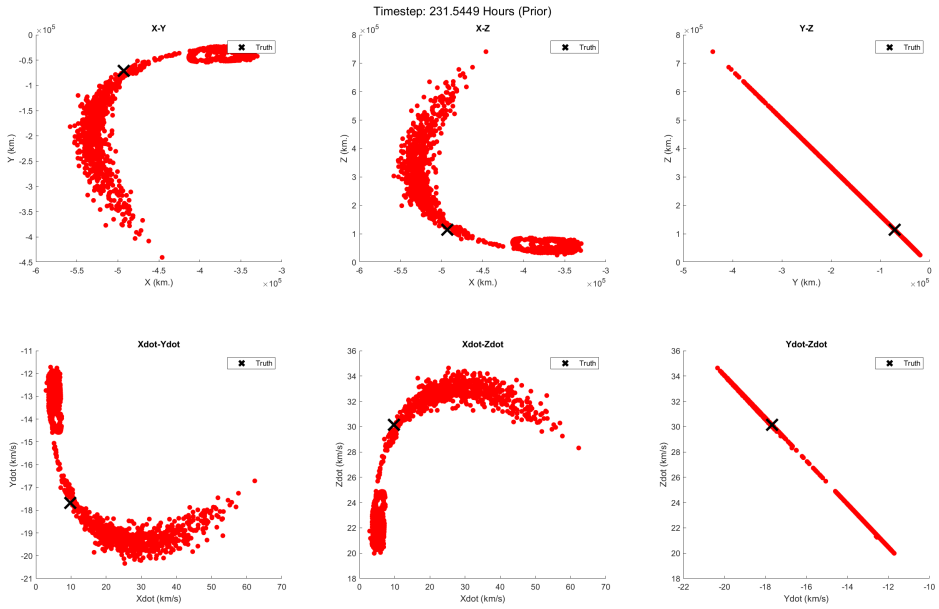

Figure 10: Distribution of particles after 8 days of continuous propagation, with a small bifurcation resulting into two orbit families

wish to study the utility of this framework on orbit families which bifurcate into the orbit sub-

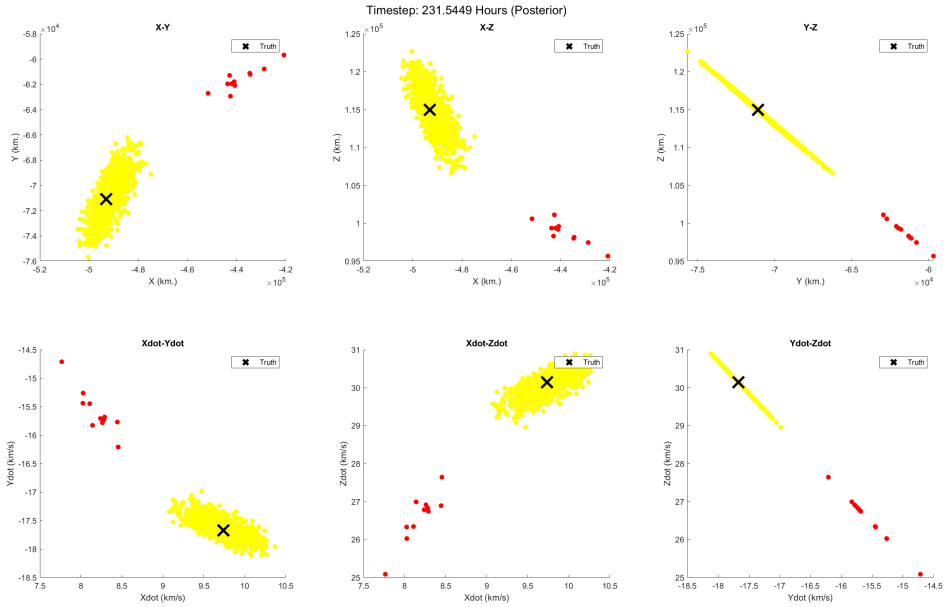

Figure 11: Starting with the distribution in Figure 10, the PGM clustering and update step results in a posterior distribution in which one cluster (the one which contains the truth) dominates.

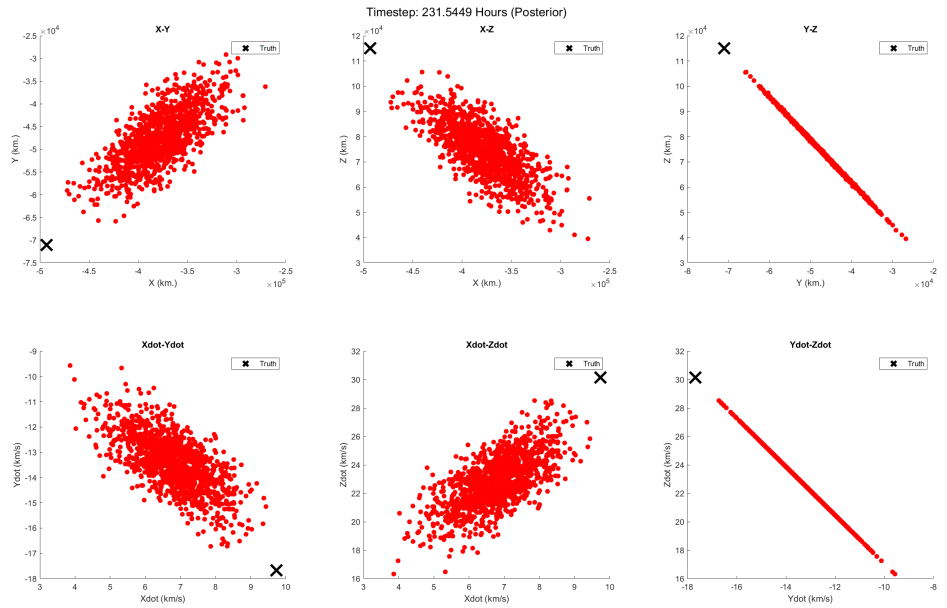

Figure 12: Starting with the distribution in Figure 10, the EnKF update step results in a posterior distribution in which we immediately lose track of the target.

families shown in Refs. [17], [18], and [19]. Additionally, we wish to apply the multi-object tracking strategies proposed in *Mishra et. al. 2023* to sets of targets in cislunar space.[20] Finally, we wish to study the utility of our combined IOD-OD framework with more complex dynamics models such as the general restricted three-body problem (R3BP).

ACKNOWLEDGMENT

The authors of this paper are grateful to the United States Space Force (USSF) Chief Technology and Innovation Office for funding this project.

REFERENCES

[1] *National Cislunar Science Technology Strategy*. Washington, DC: National Science and Technology Council, 1st ed., 2022.

[2] R. Gooding, "A New Procedure for the Solution of the Classical Problem of Minimal Orbit Determination from Three Lines of Sight," *Celest. Mech. Dyn. Astron.*, Vol. 66, No. 4, 1997, pp. 387–423.

[3] L. Taff, "ON GAUSS'S METHOD OF ORBIT DETERMINATION," tech. rep., Massachusetts Institute of Technology Lincoln Laboratory, 06 1979.

[4] K. J. DeMars and M. K. Jah, "Probabilistic Initial Orbit Determination Using Gaussian Mixture Models," *Journal of Guidance, Control, and Dynamics*, Vol. 36, No. 5, 2013, pp. 1324–1335, 10.2514/1.59844.

[5] M. S. Tom Kelecy and M. Jah, "APPLICATION OF THE CONSTRAINED ADMISSIBLE REGION MULTIPLE HYPOTHESIS FILTER TO INITIAL ORBIT DETERMINATION OF A BREAK-UP," *Proceedings of the 6th European Conference on Space Debris*, 2013.

[6] M. P. W. Islam I. Hussein, Christopher W.T. Roscoe and J. Paul W. Schumacher, "Probabilistic Admissibility in Angles-Only Initial Orbit," *Proceedings of the 24th International Symposium on Space Flight Dynamics, Laurel, MD*, 2014.

[7] M. P. W. Islam I. Hussein, Christopher W.T. Roscoe and J. Paul W. Schumacher, "Probabilistic Admissible Region for Short-Arc Angles-Only Observations," *Proceedings of the Advanced Maui Optical and Space Surveillance Technologies Conference, Wailea, HI*, 2014.

[8] U. R. Mishra, S. Chakravorty, W. R. Faber, I. I. Hussein, S. G. Hesar, and B. Sunderland, "Geometric Solution to Probabilistic Admissible Region (PAR)," *The Journal of the Astronautical Sciences*, 2024.

[9] D. H. B. R. S. Mark Bolden, Dr. Islam Hussein and D. E. Griggs, "Probabilistic Initial Orbit Determination and Object Tracking in Cislunar Space Using Optical Sensors," *Proceedings of the Advanced Maui Optical and Space Surveillance Technologies Conference, Wailea, HI*, 2022.

[10] D. I. H. M. B. K. C. Dr. Erin Griggs, Matt Schierholtz and D. H. Borowski, "Probabilistic Initial Orbit Determination and Object Tracking in Cislunar Space Using Passive Radio Frequency Sensors," *Proceedings of the Advanced Maui Optical and Space Surveillance Technologies Conference, Wailea, HI*, 2023.

[11] M. Hejduk, "Specular and Diffuse Components in Spherical Satellite Photometric Modeling," *Proceedings of the Advanced Maui Optical and Space Surveillance Technologies Conference, Wailea, HI*, 2013.

[12] D. Raihan and S. Chakravorty, "Particle Gaussian mixture filters-I," *Automatica*, Vol. 98, 2018, pp. 331–340, https://doi.org/10.1016/j.automatica.2018.07.023.

[13] H. Schaub and J. L. Junkins, *Analytical Mechanics of Space Systems*. Reston, VA: AIAA Education Series, October 2003, 10.2514/4.861550.

[14] L. P. J. C. I. T. C. J. F. M. I. R. L. M. L. T. S. John Carrico Jr., Donald Dichmann and R. Sherman, "Lunar-Resonant Trajectory Design for the Interstellar Boundary Explorer (IBEX) Extended Mission," *Proceedings of the AAS/AIAA Astrodynamics Specialist Conference, Girdwood, AK*, 2011.

[15] R. L. . J. P. C. J. Donald J. Dichmann, "Dynamics of Orbits Near 3:1 Resonance in the Earth-Moon System," *Journal of Astronautical Sciences*, Vol. 60, 2013, pp. 51–86, https://doi.org/10.1007/s40295-014-0009-x.

[16] S. Lloyd, "Least squares quantization in PCM," *IEEE Transactions on Information Theory*, Vol. 28, No. 2, 1982, pp. 129–137, 10.1109/TIT.1982.1056489.

[17] D. Grebow, "GENERATING PERIODIC ORBITS IN THE CIRCULAR RESTRICTED THREEBODY PROBLEM WITH APPLICATIONS TO LUNAR SOUTH POLE COVERAGE," Master's thesis, Purdue University, 2006.

[18] E. M. Zimovan, "CHARACTERISTICS AND DESIGN STRATEGIES FOR NEAR RECTILINEAR HALO ORBITS WITHIN THE EARTH-MOON SYSTEM," Master's thesis, Purdue University, 2017.

[19] E. M. Z. Spreen, *TRAJECTORY DESIGN AND TARGETING FOR APPLICATIONS TO THE EXPLORATION PROGRAM IN CISLUNAR SPACE*. Phd thesis, Purdue University, West Lafayette, IN, May 2021. Available at `https://engineering.purdue.edu/people/kathleen.howell.1/Publications/Dissertations/2021_ZimovanSpreen.pdf`.

[20] I. I. H. W. F. S. H. B. S. Utkarsh R. Mishra, Suman Chakravorty, "Comparing Traditional and Admissible-Region Schemes For Angles-Only Initial Orbit," *Proceedings of the Advanced Maui Optical and Space Surveillance Technologies Conference, Wailea, HI*, 2023.